Luminescence of a GaN grain with a nonpolar and semipolar plane in relation to microstructural characterization*

Zhou Xiao-Wei(周小伟)[a)b)], Xu Sheng-Rui(许晟瑞)[a)†], Zhang Jin-Cheng(张进成)[a)], Dang Ji-Yuan(党纪源)[c)], Lü Ling(吕 玲)[a)], Hao Yue(郝 跃)[a)], and Guo Li-Xin(郭立新)[b)]

[a)] *Key Laboratory of Wide Band-Gap Semiconductor Technology, School of Microelectronics, Xidian University, Xi'an* 710071, *China*

[b)] *School of Science, Xidian University, Xi'an* 710071, *China*

[c)] *Flight Automatic Control Research Institute, AVIC, Xi'an* 710065, *China*

(Received 6 December 2011; revised manuscript received 1 March 2012)

We report on the growth of the high-quality GaN grain on a *r*-plane sapphire substrate by using a self-organized SiN interlayer as a selective growth mask. Transmission electron microscopy, scanning electron microscopy, and Raman spectroscopy are used to reveal the effect of SiN on the overgrown *a*-plane GaN growth. The SiN layer effectively terminates the propagation of the threading dislocation and basal plane stacking faults during *a*-plane GaN regrowth through the interlayer, resulting in the window region shrinking from a rectangle to a "black hole". Furthermore, strong yellow luminescence (YL) in the nonpolar plane and very weak YL in the semipolar plane on the GaN grain is revealed by cathodoluminescence, suggesting that C-involved defects are responsible for the YL.

Keywords: nonpolar, semipolar, GaN, yellow luminescence

PACS: 78.55.Cr, 81.15.Kk **DOI:** 10.1088/1674-1056/21/6/067803

1. Introduction

Gallium nitride and its alloys with aluminum and indium are very attractive materials especially due to their wide application in electronic and optoelectronic devices. The majority of conventional GaN devices are grown with respect to the *c* plane. The polarization fields in multiple quantum well structures along the polar *c* axis cause significant band bending, thus giving rise to the spatial separation of electrons and holes. This situation leads to a reduced optical emission efficiency of light-emitting diodes (LEDs), as well as an undesirable redshift in the emission spectra from the quantum wells.[1] One approach to try and solve this problem is to grow a nonpolar *m*-plane or *a*-plane hexagonal GaN.[2−6] These kind of GaN devices can provide not only the high performance of an LED, such as in optical output power and wavelength ranges, but also give some unique functions such as polarized light emission, which will be explored as a new field of application.[7]

There have been reports that the nonpolar GaN layers based on heteroepitaxial growth exhibit dislocations of around $\sim 10^{10}$ cm^{-2} and basal plane stacking faults (BSFs) of around $\sim 10^{6}$ cm^{-1} in a certain range of growth conditions.[8−10] Such a high defect density is believed to restrict the internal quantum efficiency of the InGaN/GaN heterostructure at room temperature. So far, the best nonpolar performance of an LED with a much lower density of defects and stacking faults has been achieved by using the epitaxial growth on an expensive bulk GaN substrate.[11−14] Although high-quality GaN substrates with arbitrary orientations are available commercially, they are small in size, high in cost, and limited in production volume, thus, they are unsuited for commercial LED production. Therefore, to realize low-cost nonpolar GaN devices with high efficiencies, the defect density of heteroepitaxial nonpolar GaN film must be reduced.[15] So the defect-reduction technique epitaxial lateral overgrowth (ELOG) is widely used in non-

*Project supported by the Fundamental Research Funds for the Central Universities, China (Grant No. K50511250002), the National Key Science and Technology Special Project, China (Grant No. 2008ZX01002-002), and the National Natural Science Foundation of China (Grant Nos. 60736033, 60976068, and 61076097).

†Corresponding author. E-mail: shengruixidian@126.com

© 2012 Chinese Physical Society and IOP Publishing Ltd

polar GaN.[16−18] Even using the ELOG technique, the well-known YL band centred at 2.2 eV–2.3 eV in the luminescence spectrum is still very strong.[16,17] The defect-related YL emission is an important deep level phenomenon in GaN. However, the origin of the deep acceptors responsible for the YL has still not been identified.[19−21] In fact, comparison of the luminescence properties between different polar planes of GaN with the same growth conditions will probably be helpful to further seek the intrinsic mechanism of impurity incorporation of the YL band in GaN from a different view.

In this paper, we grow high crystalline nonpolar GaN grain with a semipolar plane on a low-cost sapphire substrate with a self-organized SiN interlayer. By using this technique, the high dislocation window region shrinks from a rectangle of the traditional ELOG to a "black hole". The optical properties are examined using room temperature scanning electron microscopes (SEM), cathodoluminescence (CL) measurements and Raman spectroscopy. The microstructure and defect density of the GaN grains grown on a r-plane sapphire are investigated by transmission electron microscopy (TEM) and Raman spectroscopy.

2. Experimental procedure

In this work, the growth of a-plane GaN films was realized on r-plane $(1\bar{1}02)$ sapphire substrates using a cold-wall shower head metal–oxide chemical vapor deposition (MOCVD) system. After chemical cleaning, the r-plane sapphire substrates were loaded into the chamber. Hydrogen was used as the carrier gas and triethylgallium, trimethylaluminium, and ammonia (NH_3) were used as source compounds. Details of the growth conditions, structure, and properties of the a-plane GaN growth have been previously published.[6,22] After the growth of the template, plasma-enhanced chemical vapour deposition (PECVD) was used to deposit SiO_2 on the as-grown a-plane GaN, which served as the regrowth mask. In contrast to the conventional mask pattern techniques, the time during which SiO_2 was deposited was very short (10 s), and only some parts of the template surface were covered by the thin SiO_2, forming the self-organized SiO_2 mask without a photolithography process. Then, an 8-μm thick GaN was grown on the top of the patterned surface, resulting in an ELO layer over the SiN mask stripes.

3. Results and discussion

As has been shown for laterally overgrown c-plane GaN, the crystallographic orientation of the mask stripe openings dictates the facets and the characteristics of the lateral overgrowth.[18] Figure 1 shows an SEM image demonstrating the plan view of the sample with the 10-s SiN interlayer. One can see that most of the overgrown GaN grains aligned along the c axis. It should be noted that for the conventional ELOG on the a-plane GaN, the most effective stripe orientation of SiN is along the m axis to facilitate the GaN growth along the c axis. The self-organized SiN could promote the overgrowth along the c axis, greatly reducing the process complexity and the cost.

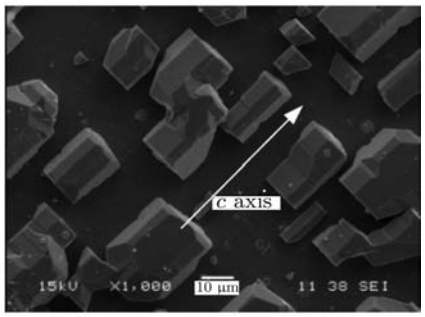


Fig. 1. Plan view SEM image showing the GaN grain aligned along the c axis.

In order to investigate spatial variations in stress and crystalline quality in the ELOG GaN structure, we performed micro-Raman mapping measurements on a single GaN grain. Spatial mapping of the E_2 (high) phonon mode provides useful information about crystalline quality and stress in the ELOG GaN structure. Micro-Raman line-scan measurements were performed above the sample surface along the direction perpendicular to the m axis orientation, at room temperature in a backscattering geometry. An argon laser of 514-nm wavelength was used to excite the sample surface through an optical microscope with a spatial resolution better than 1 μm. Figure 2 shows the full width at half maximum (FWHM) map of the E_2 (high) phonon mode, the contrast in FWHM between the wing and window regions is clearly visible. The most striking feature of the overgrown a-plane GaN is that the area of the high dislocation window region shrinks from a rectangle to a "black hole". Correspondingly, the area of the window region with the high-density defect greatly decreases. Here, one can see that the growth reveals the symmetry in lateral overgrowth rates along the m-axis direction, however,

the growth along the c-axis direction shows asymmetric character. As expected, the Ga-face sidewall grows faster than the N-face sidewall, as Imer *et al.*[23] reported that the Ga-face growth rate was 10 times faster than the N-face growth rate, but the growth rate ratio is ~ 2 for our samples, which suggests that the ratio is significantly influenced by the growth condition.

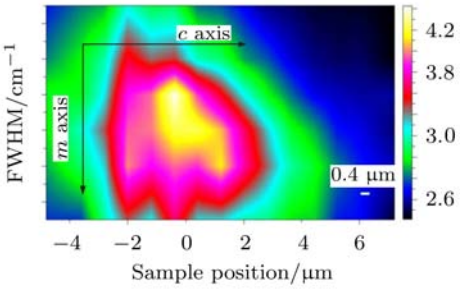


Fig. 2. (colour online) E_2 (high) phonon linewidth changes as a function of the sample position of a single GaN grain.

Moreover, as seen in Fig. 3, compared with the bulk value of 568 cm^{-1} at room temperature,[24] most of the peak values are shifted upward, indicating that the GaN layer is subjected to a compressive stress as expected in GaN growth on sapphire substrates.[25] Additionally, the high strain region is around the tiny window region. It should be noted that the window region has the highest dislocation density, at the same time it shows a few peak values are shifted upwards, indicating that the GaN layer is subjected to a little compressive stress, so the strain around the window should be associated with the interaction between the ELOG, GaN and the SiN interlayer during the overgrowth. Furthermore, one can find that the Ga-face region represents a relaxation of strain accompanied with the growth along the c axis, which is attributed to the energetic c axis being along the in-plane overgrowth direction. However, we insist that the stress state is very low according to the Raman shift of the E_2 high phonon energy, despite the stress existing in most of the overgrown regions.

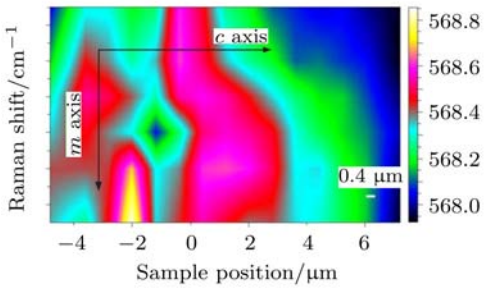


Fig. 3. (colour online) E_2 (high) phonon energy changes as a function of the sample position of a single GaN grain.

In order to further identify the effect of the SiN interlayer on the GaN grain, TEM samples were prepared by being mechanically polished before an ion beam thinned them to electron transparency, and then the microstructure of the lateral overgrowth cross-section was studied by a JEOL 2000FX TEM operating at 200 kV. The image in Fig. 4(a) is viewed along $[1\bar{1}00]$ using $g = 0002$, so partial dislocations, $a + c$ threading dislocations (TDs), and c-TDs are in contrast. It is found that the dislocation density of the nonpolar a-plane GaN template is very high below the interlayer. However, after blocking the very thin self-organized SiN interlayer, large dislocation-free regions are visible. BSFs are in contrast in Fig. 4(b) where $g = 1\bar{1}00$ along [0002]. It can be observed that the BSFs were also blocked by the TiN interlayer, consistent with the effect of the SiN interlayer on the TDs. BSFs are notoriously difficult to remove in nonpolar a-plane GaN and the only other process that was reported to be effective at removing BSFs in these materials is ELOG, specifically when the mask stripes are parallel to $[1\bar{1}00]$.[18] The dislocation suppressing effect from this technique will be discussed elsewhere.

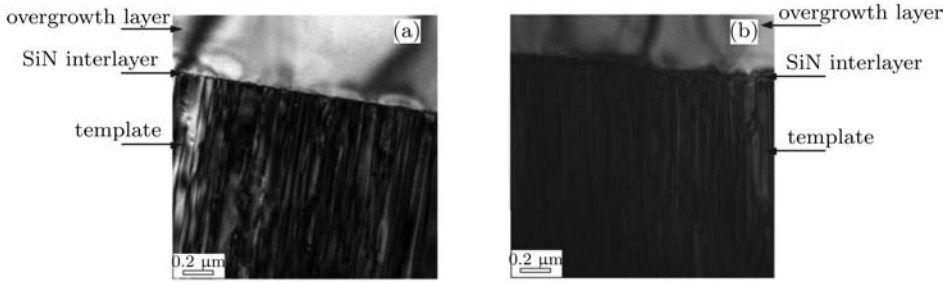


Fig. 4. Cross-sectional dark-field TEM images of sample A: (a) viewing along $[1\bar{1}00]$ using $g = 0002$ so that dislocations with a c-component are in contrast, (b) $g = [1\bar{1}00]$ so BSFs are edge-on and in contrast.

Figure 5(a) shows an SEM image of the GaN grain. There are many declining planes on the surface of the GaN grain, furthermore, the declining plane can be divided into two types: one is the plane that point B is in, this type of plane is the series nonpolar $\{11\bar{2}0\}$ plane, and the other is the semipolar plane in so-called "semipolar" orientation, in which the c axis is at an acute angle with respect to the growth a plane, i.e., the plane that point C is in Figs. 5(b) and 5(c)

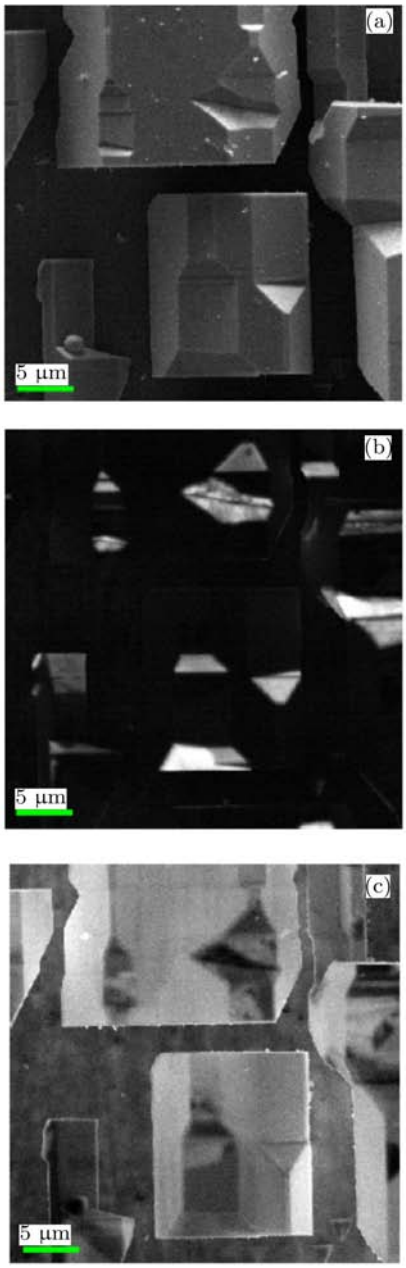


Fig. 5. (colour online) (a) SEM image of the a-plane GaN grain. CL images of the in-plane fluctuations at (b) 560 nm, (c) 364 nm, respectively.

show the monochromatic CL images of the GaN grain with emission peaks at 2.2 eV and 3.4 eV, which are attributed to YL and near band edge (NBE) emission, respectively. Comparing Figs. 5(a), 5(b), and 5(c), we see that emissions from 2.2 eV and 3.4 eV strongly complement each other, and show an extreme correlation with the crystal surface. As shown in Fig. 5(b), the YL intensities are weak in the semipolar plane, but they appear strong in the nonpolar plane, including the plane that points A and B are in. But the NBE emission is very strong in the semipolar plane.

Some authors suggest that the YL is related to the edge dislocation density.[26,27] But from the results of the TEM, we find that the density dislocation is very low, and we find the dislocations concentrate mainly in the "black hole" region as shown from the Raman result. But the strength of the YL and the dislocations do not correspond to the results of the Raman spectroscopy and the TEM, respectively. The results of the Raman spectroscopy, TEM and CL indicate that the edge dislocation has a lesser effect on the YL in GaN. Moreover, the gallium vacancy (V_{Ga}) related defect such as the V_{Ga}–O_N complex is regarded as a candidate for the deep acceptor, which will enhance the YL band, by some authors.[19,21,28] Li and Wang[28] proposed that YL-related defects may initially form or incorporate in GaN and then subsequently redistribute toward the surface during growth via a diffusion-related mechanism.[28] However, if the gallium vacancies redistribute toward the surface and play an important role in the YL, the surface of the GaN grain will be uniform. So there must be another origin for the YL. The unintentional impurities, the carbon elements, in the GaN films grown on the c-plane and r-plane as well as the m-plane sapphires by MOCVD were investigated, and the different trends of the incorporation of carbon have been explained in the polar (0001), nonpolar $(11\bar{2}0)$, and semipolar $(11\bar{2}2)$ GaN by the combination of the atom bonding structure and the origin direction of the impurities.[22] Generally, the metal–organic precursor, for example, the metal source of trimethylgallium $Ga(CH_3)_3$ will inevitably introduce carbon impurities into GaN during the overgrowth. Furthermore, in previous studies of hydride metal–organic vapour phase nonpolar a-plane GaN epilayers, we found that the YL is very weak even in the low crystalline quality a-plane GaN film. We believe that it is ascribed to the lack of carbon. So the carbon and carbon-related defects are the origin of the deep levels of YL. The different YL features of the GaN grain should be associated with the different capacities of impurity incorporated in differ-

ent planes.

4. Conclusions

In this paper, we proposed a simple technique to grow high-quality a-plane GaN grain on a r-plane sapphire with a low number of defects by using an interlayer of self-organized SiN as a dislocation filtering dielectric growth mask. Compared with conventional epitaxial lateral overgrowth schemes in the a-plane GaN, this technique exhibits an excellent effect without requiring expensive lithographic patterning steps or equipment. Furthermore, it is found that stronger YL is in the nonpolar plane and very weak YL is in the semipolar plane on the GaN grain revealed by CL, and by comparing the results of TME, Raman spectroscopy and CL, the effects of gallium vacancies and dislocations on YL are excluded, suggesting that C-involved defects are the origin of the YL.

References

[1] Waltereit P, Brandt O, Trampert A, Grahn H T, Menniger J, Ramsteiner M, Reiche M and Ploog K H 2000 *Nature* **406** 865

[2] Xu S R, Hao Y, Zhang J C, Zhou X W, Cao Y R, Ou X X, Mao W, Du D C and Wang H 2010 *Chin. Phys.* B **19** 107204

[3] Xu S R, Hao Y, Zhang J C, Xue X Y, Li P X, Li J T, Lin Z Y, Liu Z Y, Ma J C, He Q and Lü L 2011 *Chin. Phys.* B **20** 107802

[4] Xu S R, Hao Y, Zhang J C, Zhou X W, Yang L A, Zhang J F, Duan H T, Li Z M, Wei M, Hu S G, Cao Y R, Zhu Q W, Xu Z H and Gu W P 2009 *J. Cryst. Growth* **311** 3622

[5] Kim K C, Schmidt M C, Wu F, McLaurin M B, Hirai A, Nakamura S, DenBaars S P and Speck J S 2008 *Appl. Phys. Lett.* **93** 142108

[6] Xu S R, Hao Y, Yang L A, Zhang J C, Xue J S, Xue X Y, Liu Z Y, Lin Z Y, Ma J C, Li P X, Li J T and He Q 2011 *Jpn. J. Appl. Phys.* **50** 115502

[7] Masui H, Nakamura S, DenBaars S P and Mishra U K 2010 *IEEE. Electron Dev.* **57** 88

[8] Cho Y S, Sun Q, Lee I H, Ko T S, Yerino C D, Han J, Kong B H, Cho H K and Wang S 2008 *Appl. Phys. Lett.* **93** 111904

[9] Haskell B A, Wu F, Craven M D, Matsuda S, Fini P T, Fujii T, Fujito K, DenBaars S P, Speck J S and Nakamura S 2003 *Appl. Phys. Lett.* **83** 644

[10] Ma B, Hu W, Miyake H and Hiramatsu K 2009 *Appl. Phys. Lett.* **95** 121910

[11] Okamoto K, Ohta H, Nakagawa D, Sonobe M, Ichihara J and Takasu H 2006 *Jpn. J. Appl. Phys.* **45** 197

[12] Yamada H, Iso K, Saito M, Masui H, Fujito K, DenBaars S P and Nakamura S 2008 *Appl. Phys. Expr.* **1** 041101

[13] Liu J P, Lim J B, Ryou J H, Yoo D, Horne C A, Dupuis R D, Wu Z H, Fischer A M, Ponce F A, Hanser A D, Liu L, Preble E A and Evans K R 2008 *Appl. Phys. Lett.* **92** 011123

[14] Detchprohm T, Zhu M, Li Y, Xia Y, Wetzel C, Preble E A, Liu L, Paskova T and Hanser D 2008 *Appl. Phys. Lett.* **92** 109

[15] Johnston C F, Moram M A, Kappers M J and Humphreys C J 2009 *Appl. Phys. Lett.* **94** 161109

[16] Özgür Ü, Ni X, Fu Y, Morkoç H and Everitt H O 2006 *Appl. Phys. Lett.* **89** 262117

[17] Huang J J, Shen K C, Shiao W Y, Chen Y S, Liu T C, Tang T Y, Huang C F and Yang C C 2008 *Appl. Phys. Lett.* **92** 231902

[18] Craven M D, Lim S H, Wu F, Speck J S and DenBaars S P 2002 *Appl. Phys. Lett.* **81** 1201

[19] Mickevièius J, Aleksiejunas R, Shur M S, Sakalauskas S, Tamulaitis G, Fareed Q and Gaska R 2005 *Appl. Phys. Lett.* **86** 041910

[20] Neugebauera J and Walle C V 1996 *Appl. Phys. Lett.* **69** 503

[21] Xu F J, Shen B, Lu L, Miao Z L, Song J, Yang Z J, Zhang G Y, Hao X P, Wang B Y, Shen X Q and Okumura H 2010 *J. Appl. Phys.* **107** 023528

[22] Xu S R, Hao Y, Zhang J C, Cao Y R , Zhou X W, Yang L A, Ou X X, Chen K and Mao W 2010 *J. Cryst. Growth* **312** 3521

[23] Imer B, Wu F, Speck J S and DenBaars S P 2007 *J. Cryst. Growth* **306** 330

[24] Wang K R, Ramsteiner M, Mauder C, Wan Q, Hentschel T, Grahn H T, Kalisch H, Heuken M, Jansen R H and Trampert A 2010 *Appl. Phys. Lett.* **96** 231914

[25] Song J S, Rho H, Jeong M S, Ju J W and Lee I H 2010 *Phys. Rev.* B **81** 233304

[26] Grazzi C, Strunk H P, Castaldini A, Cavallini A, Schenk H P D and Gibart P 2006 *J. Appl. Phys.* **100** 073711

[27] Zhao D G, Jiang D S, Hui J J, Zhu Y, Liu Z S, Zhang S M, Liang J W, Li X, Li X Y and Gong H M 2006 *Appl. Phys. Lett.* **88** 241917

[28] Li Q M and Wang G T 2006 *Nano Lett.* **10** 1554